Int J Earth Sci (Geol Rundsch) (2017) 106:2189–2202
DOI 10.1007/s00531-016-1422-0

ORIGINAL PAPER

Post-emplacement kinematics and exhumation history of the Almora klippe of the Kumaun–Garhwal Himalaya, NW India: revealed by fission track thermochronology

Paramjeet Singh[1] · **R. C. Patel**[2]

Received: 8 May 2016 / Accepted: 30 October 2016 / Published online: 19 November 2016

Abstract Tectonically transported crystalline thrust sheet over the Lesser Himalayan meta-sedimentary zone along the Main Central Thrust (MCT) is represented by Almora, Baijnath, Askot and Chiplakot crystalline klippen. The Almora–Dadeldhura klippe in the Kumaun–Garhwal and western Nepal Himalaya is the witness and largest representative of these crystalline klippen, south of MCT. Here, we investigate the post-emplacement kinematics and exhumation history of the Almora klippe. The newly derived zircon fission track (ZFT) ages combined with published apatite fission track (AFT), ^{40}Ar–^{39}Ar ages from the Almora–Dadeldhura klippe and Ramgarh thrust sheet to quantify the temporal variation in cooling ages and exhumation rates. Using 1-D numerical modelling approach, we calculate the transient exhumation rates with respect to different time intervals. New ZFT cooling ages along ~50-km-long orogeny perpendicular transect across the Almora klippe range between 13.4 ± 0.6 and 21.4 ± 0.9 Ma. Published AFT ages and ^{40}Ar–^{39}Ar ages from the Almora–Dadeldhura klippe range 3.7 ± 0.8–13.2 ± 2.7 and 18.20–25.69 Ma, respectively. AFT ages reported from Ramgarh thrust sheet range 6.3 ± 0.8–7.2 ± 1.0 Ma in Kumaun region and 10.3 ± 0.5–14.4 ± 2.2 Ma in western Nepal. The linear age trend along with youngest ZFT age (~14 Ma) close to the North Almora Thrust (NAT) in its hanging wall suggests rapid uplift close to the NAT due to its reactivation as back thrust. The transient exhumation rates of Almora klippe agree that the erosion rate was rapid (0.58 mma^{-1}) close to the NAT in its hanging wall and relatively slow (0.31 mma^{-1}) close to the SAT in its hanging wall during 15–11 Ma. We interpret that the fission track ages and transient exhumation rate pattern of crystalline klippen show a dynamic coupling between tectonic and erosion processes in the Kumaun–Garhwal Himalaya. However, the tectonic processes play the major role in controlling the exhumation pattern.

Keywords Exhumation · Fission track ages · Almora klippe · Lesser Himalayan Crystalline · Kumaun–Garhwal Himalaya

Introduction

Thermochronology of apatite and zircon allows to determine the timing, exhumation and rate of cooling of rocks from a temperature range ~250 to ~110 °C (Naeser 1979; Reiner's et al. 2004, 2005). In the collisional mountain belts like almighty Himalaya, it is not clear that how the temperature–time path/cooling ages linked with active folding, faulting and erosional processes. The exact correlation of age and rate of displacement of thrust/fault are still most challenging problem in the evolution of a collisional mountain belt. We should address how the rocks cool/exhume and transport. What factors are controlling the erosion rates and the impact of tectonics and climate over these surface processes?

The Himalayan orogeny is the result of continent–continent collision between Indian and Eurasian plate that began ~55 Ma (reviews in Hodges 2000). Due to this convergence, the hundreds of kilometres shortening have been accommodated throughout the Himalaya, which caused the

✉ Paramjeet Singh
psinghgeol@gmail.com

[1] Wadia Institute of Himalayan Geology, 33, GMS Road, Dehradun 248001, India

[2] Department of Geophysics, Kurukshetra University, Kurukshetra 136119, India

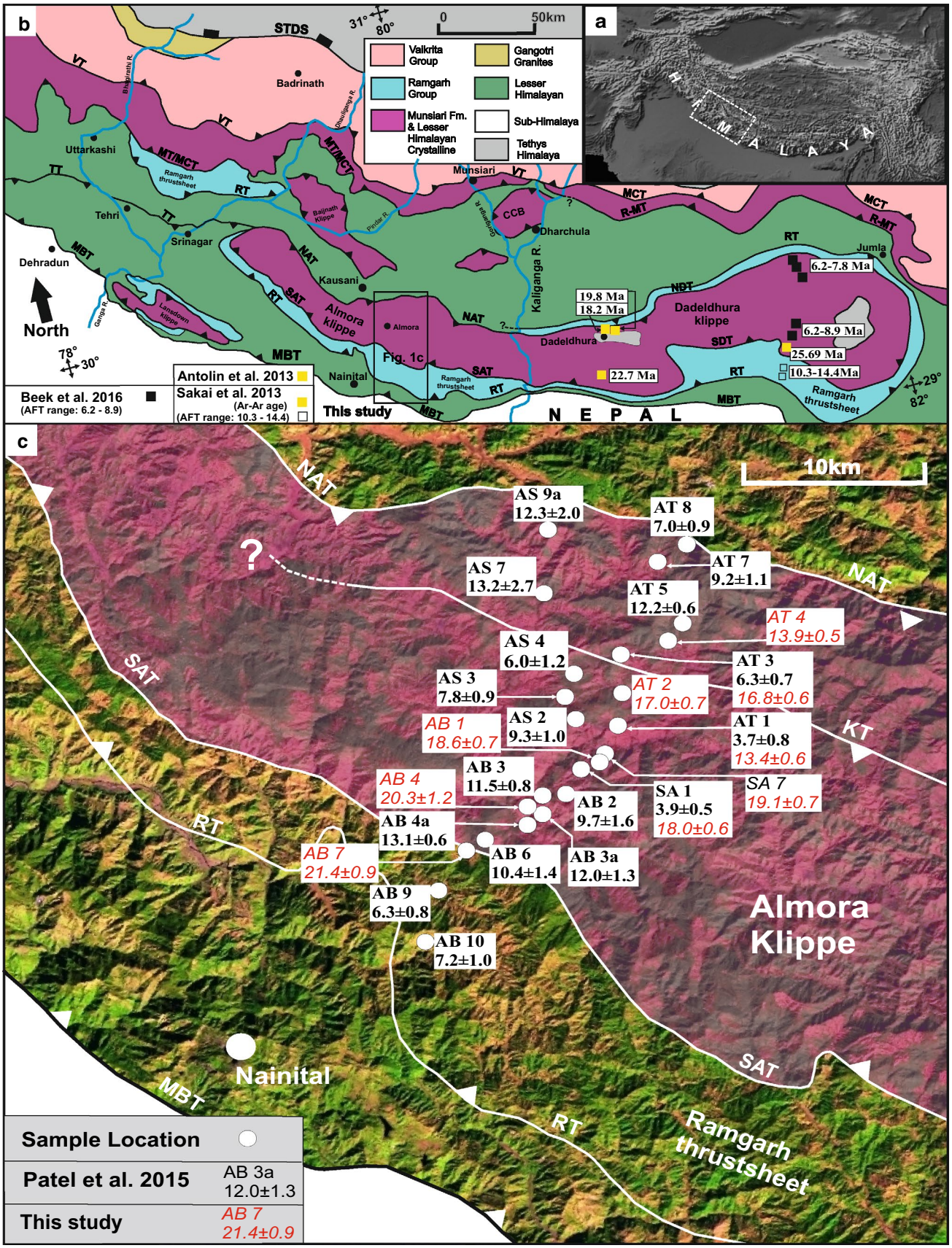
b
STDS
31°
80°
0
50km
Vaikrita Group
Gangotri Granites
Ramgarh Group
Lesser Himalayan
Munsiari Fm. & Lesser Himalayan Crystalline
Sub-Himalaya
Tethys Himalaya
Badrinath
Uttarkashi
Tehri
Srinagar
Dehradun
Kausani
Almora
Nainital
Munsiari
Dharchula
Jumla
Dadeldhura
Dadeldhura klippe
Almora klippe
Ramgarh thrustsheet
Baijnath Klippe
Landoure Klippe
Fig. 1c
VT
MT/MCT
TT
RT
NAT
SAT
MBT
MCT
R-MT
CCB
NBT
SDT
Kaliganga R.
Bhagirathi R.
Dhauliganga R.
Pindar R.
Gandaghar R.
Ganga R.
North
78°
30°
29°
82°
19.8 Ma
18.2 Ma
6.2-7.8 Ma
6.2-8.9 Ma
25.69 Ma
10.3-14.4Ma
22.7 Ma
Antolin et al. 2013
Sakai et al. 2013
(Ar-Ar age)
(AFT range: 10.3 - 14.4)
Beek et al. 2016
(AFT range: 6.2 - 8.9)
This study
N E P A L
a
H I M A L A Y A
c
10km
NAT
SAT
RT
KT
MBT
?
AS 9a 12.3±2.0
AT 8 7.0±0.9
AS 7 13.2±2.7
AT 7 9.2±1.1
AT 5 12.2±0.6
AT 4 13.9±0.5
AS 4 6.0±1.2
AT 3 6.3±0.7 16.8±0.6
AS 3 7.8±0.9
AT 2 17.0±0.7
AB 1 18.6±0.7
AS 2 9.3±1.0
AT 1 3.7±0.8 13.4±0.6
AB 3 11.5±0.8
AB 4 20.3±1.2
SA 1 3.9±0.5 18.0±0.6
SA 7 19.1±0.7
AB 2 9.7±1.6
AB 4a 13.1±0.6
AB 7 21.4±0.9
AB 6 10.4±1.4
AB 3a 12.0±1.3
AB 9 6.3±0.8
AB 10 7.2±1.0
Almora Klippe
Nainital
Ramgarh thrustsheet
Sample Location
Patel et al. 2015
AB 3a 12.0±1.3
This study
AB 7 21.4±0.9

◂**Fig. 1** **a** Topography based on the GTOPO30 digital elevation model (US Geological Survey) of the Himalaya. **b** Location and physiography of the Almora–Dadeldhura klippe in Kumaun and western Nepal regions (modified after Valdiya 1980a, b; Robinson and Pearson 2006). **c** Sample location map and tectonic domains of Almora klippe in the Kumaun–Garhwal region, Uttarakhand, India. Major thrusts and tectonic boundaries are shown in *white solid lines*. *STDS* South Tibetan Detachment System, *VT* Vaikrita Thrust, *MCT* Main Central Thrust, *MT* Munsiari Thrust, *MBT* Main Boundary Thrust, *SAT* South Almora Thrust, *KT* Kasun Thrust, *NAT* North Almora Thrust, *RT* Ramgarh Thrust, *CCB* Chiplakot Crystalline Belt, *R-MT* Ramgarh–Munsiari Thrust

south-directed deformation, tectonic transport and thrusting throughout the orogeny (Molnar and Tapponier 1975; Searle et al. 1987; Srivastava and Mitra 1994; Mukherjee 2013a, 2015; Long et al. 2011; Mukherjee et al. 2012; Robinson and Pearson 2013) and back thrusting (Mukherjee 2013b). During Late Oligocene, the initiation of MCT starts the exhumation of Higher Himalayan Crystalline (HHC) and later on, the crystalline rocks of HHC transported towards south over the Lesser Himalayan Sequence (LHS) between the Main Central Thrust (MCT) at base and South Tibetan Detachment System (STDS) at top. The emplacement of crystalline thrust sheet over the LHS along the MCT initiated throughout the Himalayan orogeny during early Miocene [regionally known as Jutogh Thrust in Himachal, Munsiari Thrust (MT) in Kumaun, Ramgarh–Munsiari Thrust (R-MT) in western Nepal, Paro in Sikkim and Bomdila in western Arunachal Himalaya] (Heim and Gansser 1939; Valdiya 1962; Robinson et al. 2003, 2006; Robinson and McQuarrie 2012; Mandal et al. 2015). Southward translation of these crystalline rocks over the LHS along the MCT followed by development of the Lesser Himalayan Duplex (LHD) during Middle Miocene and produced large synclinal and anticlinal structures between the MCT and the Main Boundary Thrust (MBT) (Robinson et al. 2003, 2006; Khanal et al. 2015). Later on, these synclinal structures occur as klippen such as Almora, Baijnath, Chiplakot in Kumaun region and Dadeldhura, Kathmandu, in western Nepal contains low- to medium-grade metamorphic rocks over the Lesser Himalayan meta-sedimentary (LHMS) rocks (Fig. 1b). The Almora–Dadeldhura klippe is commonly known the southern extension of Munsiari Formation in Kumaun and Ramgarh–Munsiari Formation in western Nepal (Valdiya 1980a, b; Srivastava and Mitra 1994; Robinson et al. 2003, 2006; Khanal et al. 2015; Patel et al. 2015).

Our present knowledge on kinematics and emplacement of Lesser Himalayan Crystalline (LHC) rocks over the LHS in the south of MCT raises many geological questions. They are: how these crystalline rocks are emplaced over LHS? What is the post-emplacement tectonics and exhumation history of LHC rocks since Early Miocene? Recent studies from the Kathmandu klippe of the central Nepal have reported that the crystalline klippen rocks do not show inverted metamorphism like the HHC (Johnson et al. 2001). The Almora–Dadeldhura klippe in Kumaun and western Nepal and Kathmandu klippe in central Nepal are considered as the southern extension of Tethys Himalayan Sequence (THS) to the south of merging two thrust faults: MCT and STDS (Webb et al. 2007, 2011). Antolín et al. (2013) study from Dadeldhura region did not favour the merging of MCT and STDS at the northern base of the klippe and reported the thrust sense top-to-S shear at the base and normal sense top-to-N/NE shear at the top of the Almora–Dadeldhura klippe. The published ^{40}Ar–^{39}Ar ages (Antolín et al. 2013; Sakai et al. 2013) and AFT ages (Patel et al. 2015; van der Beek et al. 2016) from the Almora–Dadeldhura klippe revealed the timing of emplacement of crystalline thrust sheet over the LHS during Early Miocene (ca. 25–18 Ma) and post-emplacement exhumation history within 13–4 Ma, i.e. Late Miocene, respectively (Fig. 1b). In order to identify the gap in our knowledge of the exhumation history of Almora–Dadeldhura klippe, our new ZFT data will address the post-emplacement exhumation history of the Almora klippe ranging 22–13 Ma, i.e. Early to Late Miocene. We also quantify the spatial–temporal variation in exhumation rates in the specific time intervals and address the emplacement of crystalline thrust sheet, development of post-emplacement kinematics and exhumation history of the Almora–Dadeldhura crystalline sheet of Kumaun Lesser Himalaya (Fig. 1b). The cooling FT ages and 1-D modelling link with geometry and kinematics of the Almora klippe and will offer a detailed depiction of the transient exhumation rates after it emplaced over the Kumaun Lesser Himalaya.

Geology and tectonics

The Almora klippe is one of the largest and witness of crystalline thrust sheets in Kumaun–Garhwal region of NW Himalaya. Heim and Gansser (1939) described that the sub-Himalaya, Lesser Himalayan Sequence (LHS), Higher Himalayan Crystalline and Tethys Himalayan Sequence (THS) are stacked from north-dipping Main Frontal Thrust (MFT), MBT, MCT and STDS from south to north. The geology, tectonic and stratigraphy of the Kumaun–Garhwal region were well described in Valdiya (1962, 1980a, b). The rocks of the LHS are largely Precambrian meta-sedimentary units with their continuous extension and correlation of Lesser Himalayan Formation of western Nepal described by Valdiya (1986). In Kumaun, the Lesser Himalayan meta-sedimentary zone is comprised of overlying folded crystalline thrust sheet such as: Almora, Chiplakot and Baijnath klippen and Ramgarh thrust sheet (Rupke 1974; Valdiya 1980a, b; Srivastava and Mitra 1994; Célérier et al.

2009a; Patel et al. 2011b) (Fig. 1b). The Almora–Dadeldhura klippe in the footwall of the MT/MCT extends from Dudhatoli in Garhwal region to Kaliganga in Kumaun region and further east through the Dadeldhura region of western Nepal (Valdiya 1980a, b, 1986; Upreti and LeFort 1999; Arita et al. 1984; Robinson et al. 2003, 2006; Antolín et al. 2013).

In the Kumaun–Garhwal region of NW Himalaya, the LHS between the MBT at south and Munsiari Thrust (MT/MCT) at north is juxtaposed by a sequences of thrusts, some of which have been broadly folded, and some of the major regional thrust faults are like the Tons Thrust (TT), the Ramgarh Thrust (RT) and the Berinag Thrust (BT) (see Fig. 4). In Kumaun region, the NAT and SAT are described as the folded southern continuation of MT/MCT and form the crystalline Almora klippe. The Almora–Dadeldhura klippe is the asymmetrical plunging synform underlain by steeply inclined south-dipping North Almora Thrust (known as NAT in Kumaun region)/ North Dadeldhura Thrust (known as NDT in western Nepal) in the northern flank and gently north-dipping South Almora Thrust (known as SAT in Kumaun region)/ South Dadeldhura Thrust (known as SDT in western Nepal) in the southern flank. The Almora–Dadeldhura klippe tectonically overlies the Ramgarh thrust sheet, and the composite of Almora–Dadeldhura klippe and Ramgarh thrust sheet has been thrust over the LHS along the Ramgarh Thrust (RT) (Joshi 1999; Robinson et al. 2006; Mandal et al. 2015). The Almora klippe is divided into two thrust sheets by regional synclinal folded and south-dipping thrust known as the Kasun Thrust (KT), which merged underneath with the NAT (Valdiya et al. 1996; Valdiya 2001; Valdiya and Kotlia 2001; Patel et al. 2015) (Fig. 1c). The Almora klippe is characterized by medium- to high-grade metamorphic rocks of Almora Group with schists, garnetiferous mica schists and lower amphibolites of regional metamorphic. It includes concordantly plutonic bodies of granodiorites and granites (Valdiya 1980a, b; Joshi and Tiwari 2008). The underlying Ramgarh thrust sheet is actually a thrust-bound tectonic unit analogue in tectonic and lithological attributes to the Chail klippe of the Himachal Pradesh (Valdiya 1980a, b). It comprises of quartz porphyries and porphyritic granites suite occurring in a succession of phyllites, fine-grained quartzwackes, meta-siltstones and carbonaceous pyrite-bearing slates alternating with white-blue marbles of Ramgarh Group (Valdiya 1980a, b).

Previous thermochronological studies

Thermochronological studies from the Lesser Himalayan region of NW and central Himalaya are very limited due to apatite-zircon poor lithologies in the meta-sedimentary rocks of LHS. However, the Kumaun and western Nepal Himalaya have advantage that the rocks of Lesser Himalayan Crystalline klippen covering the LHS zone have good concentration of apatite and zircon. AFT studies have been carried out in the Jutogh klippe which ranges 2.2 ± 0.8–12.2 ± 1.8 Ma and suggests that thrust sheet emplaced over the LHS ~10 Ma and after that the rock upliftment and exhumation start (Thiede et al. 2009). It has been described that Almora and other crystalline thrust sheets emplaced over the LHS during Early Miocene (~24–18 Ma) (Srivastava and Mitra 1996; Célérier et al. 2009a; Antolín et al. 2013; Sakai et al. 2013). AFT ages reported by Patel et al. (2015) from the Almora klippe range 3.7 ± 0.8–13.2 ± 2.7 Ma and suggest reactivation of the south-dipping Kasun Thrust (KT) and the North Almora Thrust (NAT) as a back thrust during ~6–8 Ma. AFT ages reported from Ramgarh thrust sheet range 6.3 ± 0.8–7.2 ± 1.0 Ma and suggest that this thrust sheet exhumed faster than the Almora klippe (Patel et al. 2015). From Baijnath klippe, 3 AFT ages range 4.7 ± 0.5–6.6 ± 0.8 Ma. This indicates that the Baijnath thrust reactivated ~5–7 Ma (Singh et al. 2012). The AFT ages data obtained from the Chiplakot Crystalline Belt (CCB) by Patel et al. (2007) are divided into two age groups and state that in the north of Central Chiplakot Thrust, the AFT ages range 7.6 ± 0.6–9.8 ± 0.6 Ma, while in the southern part, the ages range 12.9 ± 1.1–17.9 ± 0.9 Ma. The lower exhumation rates (~0.3 mma^{-1}) suggest that the CCB exhumed very slowly, since it was thrust over the LHS during Early Miocene (Srivastava and Mitra 1996; Célérier et al. 2009a; Patel et al. 2007, 2015). Singh et al. (2012) reported 3 young AFT ages from Berinag Formation near the Loharkhet Village north to the Berinag Thrust (BT), which range between 0.3 ± 0.1 and 0.9 ± 0.2 Ma, and a single $^{40}Ar/^{39}Ar$ age (4.3 Ma) from Berinag Formation near the Munsiari town by Célérier et al. (2009b) suggests the reactivation of BT. The young AFT ages (<5 Ma) from Vaikrita Group, Munsiari Formation and Berinag Formation along the Dhauliganga, Pindar and Goriganga rivers suggest the reactivation of VT, MT and BT in a sequential piggy-back style (Patel and Carter 2009; Singh et al. 2012). Additionally, one AFT age of 3.6 ± 0.8 Ma from the inner LHS Zone near Kausani has been reported (Patel et al. 2015). Recent studies from the western Nepal reported that the AFT ages range between 6.2 ± 0.5 and 8.9 ± 1.5 Ma from the Dadeldhura region along the Karnali River section (van der Beek et al. 2016). Sakai et al. (2013) reported that one ^{40}Ar–^{39}Ar biotite age 25.69 ± 0.13 Ma from the Almora–Dadeldhura klippe and fission track ages along the Jumla–Surkhet section of Ramgarh thrust sheet ranges between 7.8 ± 0.2–15.4 ± 0.7 Ma (zircon) and

10.3 ± 0.5–14.4 ± 2.2 Ma (apatite), respectively. The AFT ages along N-S transects in Kathmandu klippe of the central Nepal range between 4.7 ± 0.8 and 8.6 ± 0.5 Ma (Robert et al. 2009). The ages are comparatively older than the AFT ages from HHC reported by van der Beek et al. (2016), Robert et al. (2009, 2011) and Sakai et al. (2013). The variation in cooling ages of Lesser Himalaya and Higher Himalaya has been explained by tectonically driven exhumation (van der Beek et al. 2016) and overthrusting of a crustal ramp in the Main Himalayan Thrust (MHT) (Herman et al. 2010) in western and central Nepal.

Fission track thermochronology

Analytical procedure

To constrain the exhumation pattern, we have obtained 9 zircon fission track (ZFT) ages across the Almora klippe to understand their role in exhuming the klippe after it emplaced over the LHS. Sampling was done to obtain a section across the crystalline Almora klippe and across the individual thrust sheet within the klippe to quantify their role in exhumation of Almora klippe. Sample preparation was done following the standard mineral separation method as described in Patel et al. (2015). In brief, 100 grains of good-quality and equal-sized zircon were separated from 9 samples (Table 1) by standard crushing, heavy liquid separation using bromoform ($CHBr_3$) and magnetic separation procedures. Hand-picked zircon grains were mounted in PFA® Teflon and polished for getting maximum etched surface of the grain (i.e. 4π geometry). To reveal the spontaneous track in zircon mineral surface, the etching of mounts was done in the eutectic mixture of KOH–NaOH at 240 °C for 3 h, and after that, muscovite of low-U content (<5 ppb) was used as an "external detector" to obtain the induced track densities. Thermal neutron irradiation of samples was performed in the thermal column of the FRM-II, Germany, and CN-2 uranium glass was used as neutron dosimeter. The induced track densities on external detectors (mica) were measured after etching the detectors in 48% HF at 35 °C for 5 min. The spontaneous track densities were determined on internal mineral surfaces using an Olympus BX-50 microscope with 100× dry lens and total magnification of 1250x. Zircon crystals with prismatic sections parallel to the crystallographic c-axis were chosen to measure track densities. Ages with $\pm 1\sigma$ were calculated by standard zeta method (ζ) (Hurford and Green 1983; Hurford 1990). Zeta factor of 126.44 ± 6.81 was obtained by one of the authors PS for dosimeter glass CN-2 by multiple analyses of zircon age standards.

Table 1 Zircon fission track data of Almora klippe [a]

Sr. no.	Sample code	Longitude N	Latitude E	Elevation (m)	Mineral	Number of grains	Spontaneous track density		Induced track density		Uranium (ppm)	Dosimeter		$P(\chi^2)$	Central age ± 1σ
							$\rho_s \times 10^5$ cm^{-2}	N_s	$\rho_i \times 10^5$ cm^{-2}	N_i		$\rho_d \times 10^5$ cm^{-2}	N_d	%	
1	AB-7	29°32.62′	79°32.10′	984	Zircon	31	39.53	1399	64.93	2260	462.3	5.477	2738	74.65	21.4 ± 0.9
2	AB-4	29°33.22′	79°36.43′	1065	Zircon	25	23.41	552	40.01	887	284.9	5.477	2738	97.81	20.3 ± 1.2
3	AB-1	29°35.47′	79°38.34′	1506	Zircon	24	20.16	1803	37.77	3336	269.0	5.477	2738	31.59	18.6 ± 0.7
4	SA-1	29°35.49′	79°37.13′	1088	Zircon	23	29.26	2037	55.19	3917	393.0	5.477	2738	18.64	18.0 ± 0.6
5	SA-7	29°35.40′	79°38.30′	1508	Zircon	22	31.91	1798	58.93	3256	419.6	5.477	2738	98.18	19.1 ± 0.7
6	AT-1	29°37.37′	79°40.20′	1670	Zircon	16	14.06	903	36.99	2447	250.7	5.753	2876	44.52	13.4 ± 0.6
7	AT-2	29°38.24′	79°39.63′	1686	Zircon	31	20.24	1195	43.46	2548	294.6	5.753	2876	98.42	17.0 ± 0.7
8	AT-3	29°39.57′	79°39.87′	1626	Zircon	23	21.26	1631	46.39	3526	314.5	5.753	2876	75.46	16.8 ± 0.6
9	AT-4	29°39.93′	79°42.49′	1714	Zircon	21	13.63	1263	35.51	3316	240.7	5.753	2876	56.86	13.9 ± 0.5

[a] Samples correspond to the serial number in the map; N_s is number of spontaneous track counted, N_i is number of induced track counted, N_d is number of induced tracks counted in dosimeter glass CN5. $P(\chi^2)$ is probability for obtaining χ^2 value for ν degrees of freedom, where ν = no. of crystals − 1; central age is a modal age, weighted for different precisions of individual crystals (see Galbraith 1981)

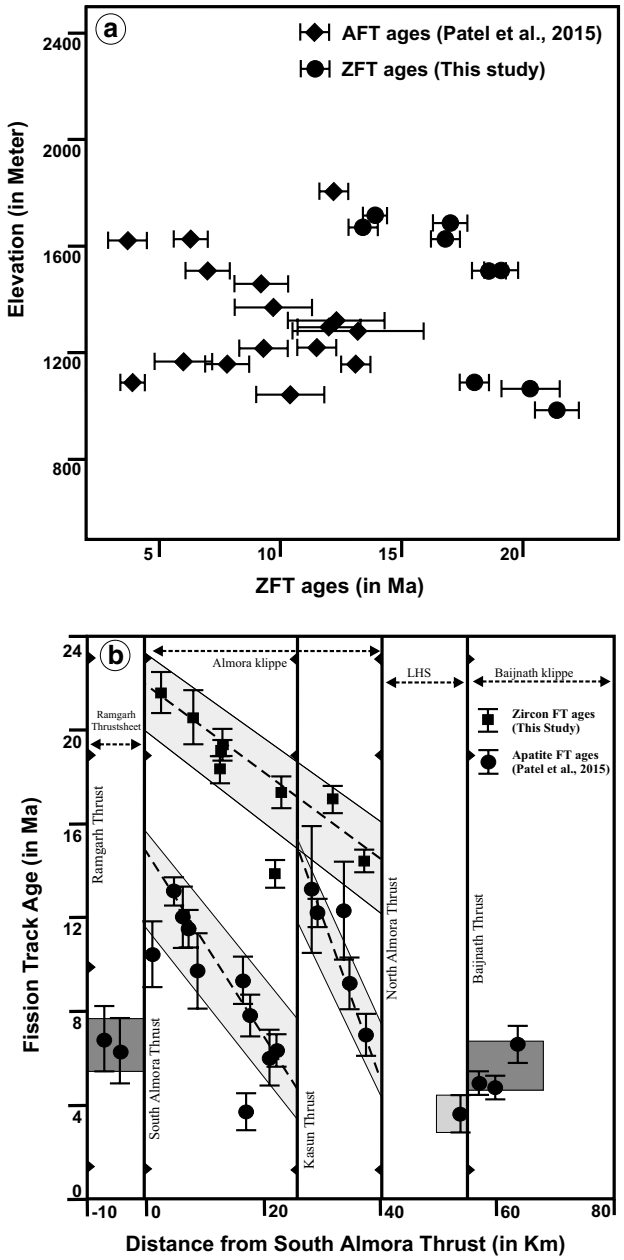

Fig. 2 **a** Fission track age versus elevation plot and **b** FT ages plotted against the horizontal distance from the South Almora Thrust (SAT) and cross section showing the tectonics along the traverse (*black dots* AFT ages, *black squares* ZFT ages)

Results

Table 1 represents the zircon fission track age data of total 9 samples from the Almora klippe. The ZFT ages from the Almora klippe range 13.4 ± 0.6–21.4 ± 0.9 Ma (Fig. 1c). The ZFT ages show a well-developed correlation with respect to tectonics of the Almora klippe and demonstrate a linearly decreasing (older to young) trend from South Almora Thrust (SAT) to North Almora Thrust (NAT) without any break in pattern across the Kasun Thrust (KT).

ZFT ages (black squares) along with published AFT ages (black circles) are plotted against the distance from South Almora Thrust (SAT) up to north of Baijnath Thrust (Fig. 2b) (Singh et al. 2012; Patel et al. 2015). The samples falling along the traverse, which are at right angle to the major tectonic boundaries, have only been considered for plotting. In this transect, the plotted ZFT ages display gradually decreasing trend from SAT to NAT without any break across the KT. The distance plot shows that ZFT ages are continuously decreasing with respect to distance towards north, with the oldest ZFT age 21.4 ± 0.9 Ma close to the SAT and youngest age 13.9 ± 0.5 Ma close to the NAT except one ZFT 13.4 ± 0.6 Ma falling slightly outside the trend near KT towards south (Fig. 2b). Similarly, the AFT ages from Almora klippe reported by Patel et al. (2015) between SAT and NAT range between 3.7 ± 0.8 and 13.2 ± 2.7 Ma and clearly indicate that AFT ages gradually decrease from SAT to NAT with a clear significant jump across the KT. The AFT ages of Almora klippe are divided into two groups: One is between SAT and KT ranging 3.7 ± 0.8–13.1 ± 0.6 Ma, and another is KT to NAT ranging between 7.0 ± 0.9 and 13.2 ± 2.7 Ma, respectively. AFT ages suggest the decreasing trend from the SAT to KT and KT to NAT with respect to distance. The younger AFT ages in the hanging wall and close proximity to KT are 6.0 ± 1.2 Ma and oldest 13.2 ± 2.7 Ma in the footwall of the KT and clearly indicate a significant jump in AFT ages. (Patel et al. 2015). The oldest AFT age in the hanging wall of SAT is 13.1 ± 0.6 Ma, and AFT ages reported from Ramgarh thrust sheet range between 6.3 ± 0.8 and 7.2 ± 1.0 Ma and also show a significant jump in the AFT ages across the SAT (i.e. the older AFT age in the hanging wall of SAT and young AFT age in footwall of SAT or the hanging wall of the RT) (Patel et al. 2015). Furthermore, AFT ages reported from the Baijnath klippe are younger: 4.7 ± 0.5–6.6 ± 0.8 Ma (Singh et al. 2012), and resemble with the AFT ages within the Ramgarh thrust sheet (see Fig. 2b).

The young AFT (3.6 ± 0.8 Ma) ages in inner LHS and Baijnath klippe also indicate the timing reactivation of inner LHD around ~4–7 Ma. To evaluate the time–elevation relation, we plot the fission track ages (new and published) of Almora klippe against the elevation profile and FT ages and elevation do not correlate (Fig. 2a).

Modelling of fission track data and transient exhumation rates

To quantify the average exhumation rates, we used 1-D (vertical) thermal modelling and explored the range of exhumation rates as used by Patel and Carter (2009), Patel

et al. (2011a) and Singh et al. (2012) in the adjacent HHC zone. Using the CLOUSER programme, the appropriate closure temperature is defined, and that value is used in AGE2EDOT programme (Brandon et al. 1998; Ehlers et al. 2005) to calculate cooling ages of AFT and ZFT thermochronometer as a function of erosion rates for samples at the mean local elevation (Brandon et al. 1998; Reiners and Brandon 2006). We used the thermal parameters of the adjacent HHC region (England et al. 1992; Roy and Rao 2000; Ray et al. 2007; Whipp et al. 2007; Thiede et al. 2009), which has the same lithology as the Almora klippe (Patel and Carter 2009; Patel et al. 2011a, b, 2015; Singh et al. 2012). The 1-D modelling is based on the geothermal gradient values ranging 30–45 °C km^{-1} (Whipp et al. 2007), thermal conductivity values of 2.1–3.6 Wm^{-1} K^{-1} (Ray et al. 2007) and for heat production the values reported by Whipp et al. (2007) ranging 0.8–3.0 μ Wm^{-1} using the maximum and minimum values.

A summary of results of transient exhumation rate from thermal modelling is present in Table 2. Our method for calculating the transient exhumation rates (Thiede et al. 2009) for each of the thermochronometer system is as follows. The mean ZFT age between NAT and KT is 15.4 Ma. To determine the exhumation rates of the zone between the NAT and KT, the mean ZFT ages (15.4 ± 2.0 Ma) suggest that the mean exhumation rate is 0.42 mma^{-1} (E_0) for the last ~15 Ma (t_0), while the mean AFT ages 10.8 ± 2.6 Ma represent the average exhumation rate 0.35 mma^{-1} (E_1) for the last ~10 Ma (t_1). Thus, the exhumation rates (E_2) between 15 and 10 Ma are given as:

$$E_2 = \left[(E_0 t_0) - (E_1 t_1)\right](t_0 - t_1)^{-1} \quad \text{(from Thiede et al. 2009)} \tag{1}$$

Now, we put the previous values of (E_0), (E_1), (t_0) and (t_1) in the above equation and suggest an exhumation rates of 0.58 mma^{-1} during ~15–10 Ma between the NAT and KT, and the exhumation rates has been reduced by almost half (from 0.58 to 0.35 mma^{-1}) since 10 Ma. A similar approach was used to obtain the exhumation rate (E_3) as a function of ^{40}Ar–^{39}Ar ages (Antolín et al. 2013) ranging between 19.8 and 18.2 Ma, with mean age 19.0 Ma. The average exhumation rate (E_0) is 0.35 for the last ~19 Ma (see Table 2) and the value of E_2 is 0.58 mma^{-1} for ~15–10 Ma and E_1 is 0.35 mma^{-1} for ~10 Ma. Therefore, the exhumation rate (E_3) is given as:

$$E_3 = [(E_0 t_0) - (E_2 t_2) - (E_1 t_1)](t_0 - t_2 - t_1)^{-1} \quad \text{(from Thiede et al. 2009)} \tag{2}$$

Equation (2) suggests an exhumation rate 0.11 mma^{-1} during ~19 and 15 Ma between the NAT and KT, which indicate that the exhumation rates have been increased by a factor of 5 from 15 Ma onwards (Fig. 3).

Table 2 Transient exhumation rates of Almora klippe

Unit between	Dating method	Total number of samples	Age (Ma)			Exhumation rates (mma^{-1})						
			Range	Mean	SD	Min	Max	Mean	SD	Duration	Corrected	$\Delta t = tx - ty$ (Ma)
North Almora Thrust (NAT)–Kasun Thrust (KT)	AFT#	5	7.0–13.2	10.8	2.6	0.25	0.45	0.35	0.14	10.8	0.35 ± 0.1 (E_1)	10.8–0
	ZFT	2	13.9–16.8	15.4	2.0	0.30	0.55	0.42	0.17	4.6	0.58 ± 0.1 (E_2)	15.4–10.8
	Ar–Ar*	2	18.2–19.8	19.0	–	0.25	0.45	0.35	–	4.4	0.11 (E_3)	19.0–15.4
Kasun Thrust (KT)–South Almora Thrust (SAT)	AFT#	11	3.7–13.2	8.5	3.2	0.45	0.65	0.55	0.18	8.5	0.52 ± 0.1 (E_1)	8.5–0
	ZFT	7	13.4–21.4	18.2	2.6	0.3	0.55	0.42	0.17	9.7	0.31 ± 0.1 (E_2)	18.2–8.5
	Ar–Ar*	2	22.8–25.7	24.2	–	0.25	0.45	0.35	–	4.6	0.06 (E_3)	24.2–18.2

AFT data: Patel et al. (2015)

* Ar–Ar data: Antolín et al. (2013) and Sakai et al. (2013) (close proximity to the respective thrusts)

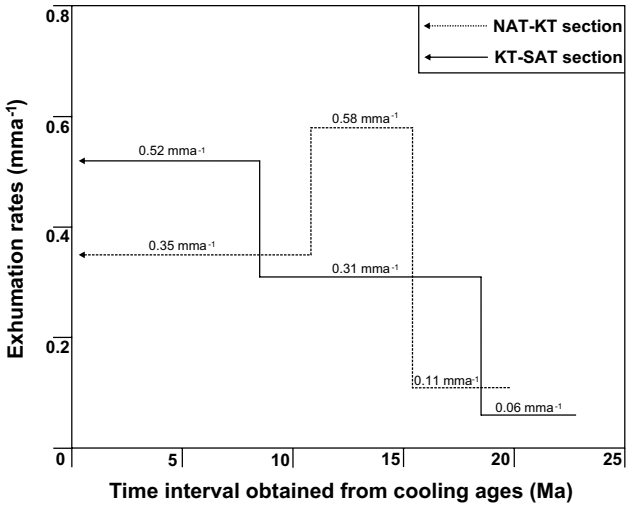

Fig. 3 Temporal variation in exhumation rates within the Almora Klippe

A similar approach was used to calculate the transient exhumation rate between KT and SAT. The mean ZFT age between SAT and KT is 18.2 Ma and suggests the average exhumation rate 0.42 mma^{-1} (E_0) for the last ~18 Ma (t_0), while the mean AFT ages 8.5 ± 3.2 Ma represent the average exhumation rate 0.55 mma^{-1} (E_1) for the last ~8 Ma (t_1). Putting these values in Eq. (1), the exhumation rate (E_2) for ~18–8 Ma is 0.31 mma^{-1} and then, it indicates that the exhumation rates have been increased by a factor of ~2 from ~8 Ma onwards probably due to the genesis of the KT around Late Miocene resulting in the rise in topography and enhanced exhumation in the hanging wall of KT. Now, we obtained (E_3) as a function of ^{40}Ar–^{39}Ar ages ranging between 25.69 and 22.7 Ma (Antolín et al. 2013; Sakai et al. 2013) with mean 24.2 Ma, put in Eq. (2) and exhumation rate is 0.06 mma^{-1} between ~25 and 18 Ma, which indicates that the exhumation rates increased by a factor 5 from 18 Ma onwards. In order to compare with precipitation in this region, we adopt the rainfall and topography relief compilation made by Bookhagen and Burbank (2006), and the data show that there is no difference in rainfall in the whole Kumaun–Garhwal region (see fig. 3c in Patel et al. 2011a). The transient exhumation rate approach has been used in the Almora–Dadeldhura klippe of Kumaon region and western Nepal region using ^{40}Ar–^{39}Ar, fission track ages reported by (this study, Antolín et al. 2013; Sakai et al. 2013; Patel et al. 2015). The mean ages close proximity to the NAT/NDT hanging wall are 19.0 Ma and close proximity to the SAT/SDT hanging wall are 24.2 Ma, which reflects the timing of emplacement of Almora–Dadeldhura klippe over the LHS during the early Miocene (Antolín et al. 2013; Sakai et al. 2013). The summary of result is given in Table 2, and temporal variation in exhumation rates with time is plotted (see Fig. 3).

Discussion

Fission track ages and exhumation pattern within the Almora klippe

The ZFT ages obtained from Almora klippe are unique and older as compared to the AFT ages of Patel et al. (2015). The AFT age data of Almora klippe show a similar range to other klippen and nappes emplaced over the LHS such as the CCB (Patel et al. 2007), the Baijnath klippe (Singh et al. 2012) and the Jutogh nappe (Thiede et al. 2009) and reveal considerable variation in exhumation rates within the Lesser Himalayan klippe. New ZFT ages revealed a very good correlation with the local tectonic setting of Almora klippe of Kumaun–Garhwal region. The ZFT ages close to NAT and SAT are 13.9 ± 0.5 and 21.4 ± 0.9 Ma, respectively. The younger ZFT ages close to NAT reflect the timing of reactivation of NAT during the inception of inner Lesser Himalayan Duplexes (LHD) around Middle Miocene and indicate that NAT behaved as a back thrust during same time. Similarly, the older ZFT ages in the SAT hanging wall reflect that no tectonic activity was recorded along SAT during Middle Miocene. The plot between horizontal distance from SAT to north of Baijnath klippe and FT ages indicate that the ZFT ages gradually decrease towards NAT in north without any break across the KT (Fig. 2b). It may be possible that when zircon mineral crossed the isotherm closer temperature (~240 °C), that time KT was not formed. The plot between horizontal distance and AFT ages reveals sharp discontinuity across the KT and highlights a step pattern of the ages within the Almora klippe (Patel et al. 2015). The significant jump with young AFT ages in hanging wall of KT reflects the formation of KT, or tectonic activity along KT was started prior to Late Miocene (~8–6 Ma). The young AFT ages (~6 Ma) in the hanging wall of KT and NAT indicate the reactivation of KT and NAT as back thrust during late Miocene (Patel et al. 2015). The AFT ages in the hanging wall and footwall of SAT is older (~13 Ma) and younger (~6 Ma) respectively. It clearly reflects that the footwall of SAT was active and was uplifting the whole Ramgarh Thrust sheet block as normal sense due to reactivation of RT.

To constrain the exhumation pattern of present study area and to know how the exhumation rates varied from early Miocene, we used 1-D thermal modelling. We calculate the transient exhumation rates, from timing of emplacement of Almora–Dadeldhura klippe over the LHS during the Early Miocene to post-emplacement exhumation pattern during Late Miocene. We use the published ^{40}Ar–^{39}Ar data (Antolín et al. 2013; Sakai et al. 2013), ZFT data (this study) and AFT data (Patel et al. 2015). The exhumation rates had been reported by Patel et al. (2015) based on only apatite thermochronometer and stated the

post-emplacement exhumation history from ~13 to 4 Ma of Almora klippe and Ramgarh thrust sheet. But here, we calculate the transient exhumation rates using ^{40}Ar–^{39}Ar, ZFT and AFT age parameters to constrain the timing of emplacement and post-emplacement exhumation history of Almora–Dadeldhura klippe from the thermal temperature range ~400 °C to surface.

The estimated transient exhumation rates are shown in Table 2. We divide the area into two tectonic zones: one from NAT to KT and another KT to SAT, and we estimate that the rocks between the zones NAT to KT were exhuming at the rate of 0.11 mma^{-1} from ~19 to 15 Ma (see Table 2; Fig. 3). After that exhumation rates accelerated due to the inception of inner LHD within the NAT zone and increased to 0.58 mma^{-1} from ~15 to 10 Ma. 10 Ma onwards the exhumation rates again slowed down and decreased up to 0.35 mma^{-1} due to the contraction and formation of KT during Late Miocene and resulting in less topography rise in NAT hanging wall (see Table 2; Fig. 3). Similarly, in the southern zone of Almora klippe, initially, the estimated exhumation rates are very low, i.e. 0.06 mma^{-1} during the period ~22–18 Ma (possibly the time of emplacement of crystalline rocks over LHMS rocks), and after that the exhumation rates are increased five times, i.e. 0.31 mma^{-1} between 18 and 8 Ma, and due to the compression, the formation of large syncline and anticline structures within the emplaced thrust sheet takes place between MBT and MCT. It results in the formation of KT during Late Miocene. Later on, after the formation of KT, the topography raised in its hanging wall and enhanced the exhumation rate up to 0.52 mma^{-1} from ~8 Ma to present day (see Fig. 3; Table 2).

Post-emplacement exhumation history of the Almora–Dadeldhura klippe

The Himalayan orogeny, developed during the Indian and Eurasian plates collision since ~55 Ma, is considered as a classic example of collisional mountain belt. In the Himalaya, exhumation is the key factor to study the processes of mountain building. Low-temperature thermochronology is the tool which infers the thermal history of a mountain belt from ~400 °C to surface (i.e. 0 °C). New ZFT age data along with published AFT data from Almora region (Patel et al. 2015) and ^{40}Ar–^{39}Ar age data (Antolín et al. 2013; Sakai et al. 2013) of white mica from Dadeldhura region inferred the timing of emplacement (i.e. 25–18 Ma) and post-emplacement kinematic and exhumation history (i.e. 18–3 Ma) of one of the largest crystalline thrust sheets of NW Himalaya between MCT in north and MBT in south over the LHS (Célérier et al. 2009a; Srivastava and Mitra 1996). The decrease in peak metamorphic temperature, pressure (400–500 °C, ~4 kbar) (Srivastava and Mitra 1994; Joshi and Tiwari 2008; Spencer et al. 2012) and older fission track age (Patel et al. 2007, 2015; Singh et al. 2012; this study) preserved towards the tip of the crystalline thrust sheet can be linked to early cooling of the Lesser Himalayan Crystalline thrust sheet, while the hinterland HHC rocks with young fission track ages (Patel et al. 2011a, b; Patel and Carter 2009; Singh et al. 2012) remained still buried, hot and underwent regional metamorphism at 7–14 kbar and 650–850 °C (Spencer et al. 2012; Rao et al. 2014). It reflects that ductile rocks constituting the HHC in depth were extruding southwards along the MCT shear zone with top-to-SW ductile shear, while the frontal crystalline thrust sheet synchronously emplaced as massive body along narrow ductile MCT shear zone over the LHS (Jain and Manikvasagam 1993; Srivastava and Mitra 1994; Godin et al. 2006; Mukherjee and Koyi 2010a, b).

Now, to constrain the post-emplacement exhumation history of Almora–Dadeldhura klippe from Early Miocene to present day, we integrate our new 9 ZFT ages combined with 15 AFT ages (Patel et al. 2015) and three ^{40}Ar–^{39}Ar ages (Antolín et al. 2013; Sakai et al. 2013) and calculated the transient exhumation rate with respect to specific time interval. Thus, we described the tectonics of Almora–Dadeldhura klippe at different time scales and its control over exhumation. The post-emplacement kinematics and exhumation history of the Almora klippe can be described as follow:

1. During the crustal shortening, the MCT which has been described as the major thrust has moved at least 80–100 km southwards (~115 km in Himachal Himalaya; 80–90 km in Kumaun–Garhwal region) (Webb et al. 2011) to emplace the ~13- to 20-km-thick crystalline thrust sheets (Almora, Baijnath, Chiplakot klippen and Ramgarh thrust sheet) on the top of the LHS meta-sedimentary rock (Fig. 4a). Southward translation along the MCT, which initiated during Late Oligocene, followed the growth of the topographic front at the leading edge of MCT hanging wall (which we assume to be the most likely location for focused denudation) (Webb 2013; Robinson and Pearson 2006; Robinson and McQuarrie 2012; Célérier et al. 2009a; Robinson et al. 2003; Webb et al. 2011; Antolín et al. 2013; Khanal et al. 2015). Later, the emplaced overlying crystalline rock folded as regional synforms and antiforms between the MCT and the MBT (Fig. 4b). This grew the topography, which exposed the anticlinal part as rapid exhumation zone due to underlying inception of Lesser Himalayan Duplex (LHD) during Middle Miocene. Similarly, the comparatively low topographic synclinal part has undergone slow exhumation, and later on, this synclinal part occurs as klippe. The

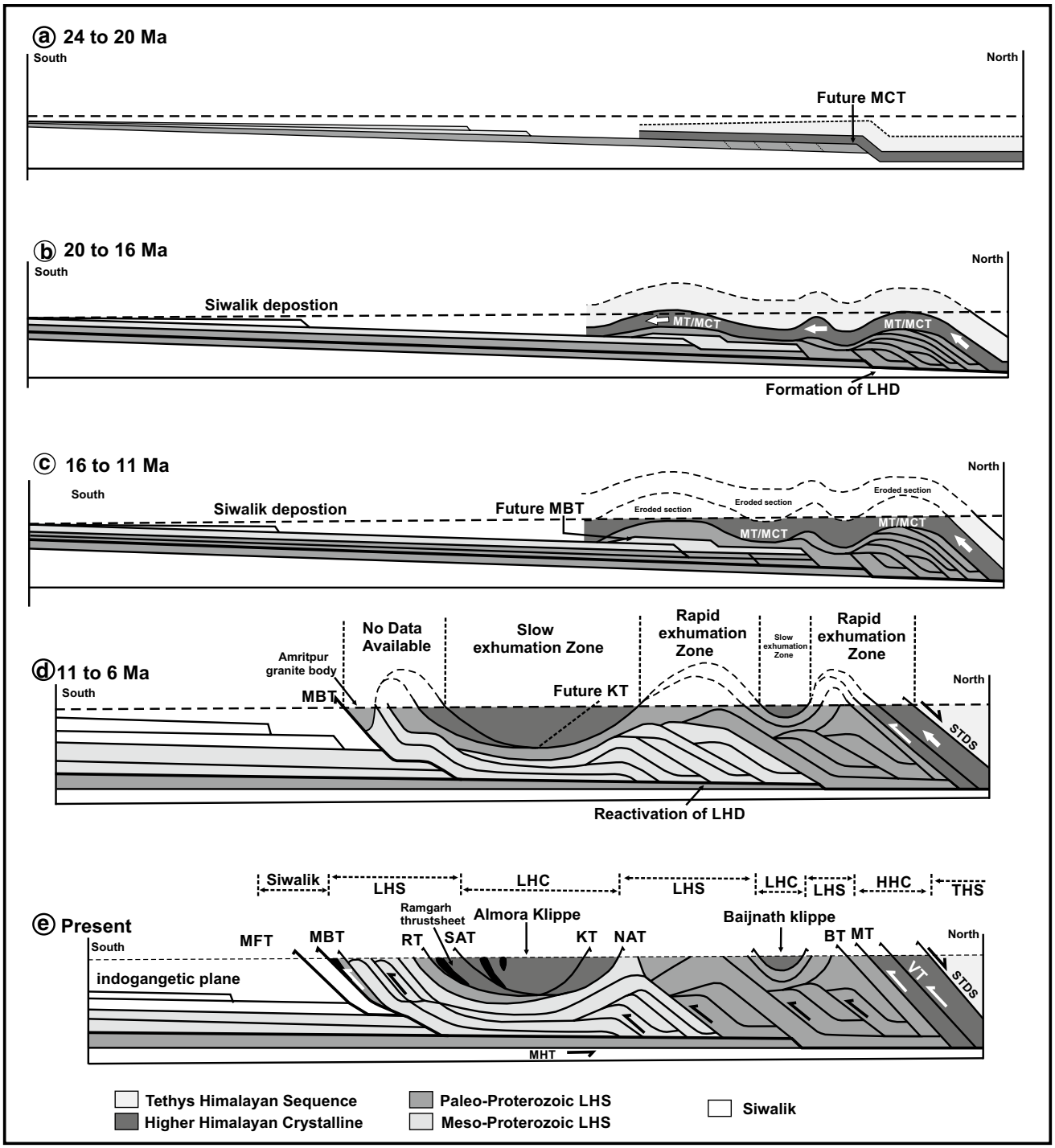

Fig. 4 Schematic model of post-emplacement kinematics and exhumation history of the Almora–Dadeldhura klippe. **a** Emplacement of crystalline rocks over the LHS along the MCT during ~24–20 Ma; **b** development of the large synclinal and anticlinal structures and inception of Lesser Himalayan Duplex (LHD) during 20–16 Ma; **c** LHD which exposed the anticlinal part as zone of rapid exhumation and synclinal part as zone of slow exhumation between 16 and 11 Ma; **d** the synclinal part of the crystalline has been eroded slowly leaving the remnant as klippe and growth of topography in hanging wall of NAT due to LHD and development of the MBT during 11–6 Ma; **e** Due to reactivation of duplexs of inner LHS zone and formation of the KT as thrust during late Miocene and showing the present tectonic setup of the Himalaya (modified after Robinson and McQuarrie 2012; Patel et al. 2015)

post-emplacement exhumation history and transient exhumation rate of Almora klippe has been calculated using ^{40}Ar–^{39}Ar, new ZFT and published AFT ages. Our result shows that the exhumation was very slow: ~0.06 and 0.11 mma^{-1} in southern and northern zone respectively (see Table 2).

2. Later during Middle Miocene, it was followed by the development of the LHD and compression due to southward propagation of MHT (Webb 2013; Robinson et al. 2003; Webb et al. 2011) (Fig. 4b, c). During Middle–Late Miocene (~18–10 Ma), the calculated transient exhumation rates increased five times (~0.3 and 0.58 mma^{-1}) in the southern and northern parts of Almora klippe, respectively (see Table 2; Fig. 3).
3. The plot of FT ages against the distance from SAT defines a systematic decrease in ZFT ages from SAT to NAT. It reflects no evidence of the KT thrust or tectonically inactive thrust fault, whereas AFT age shows a significant jump near KT. The AFT age in the hanging wall of KT is ~6 Ma, and that in footwall is ~13 Ma. It clearly reflects that the reactivation of KT or time of formation of KT as thrust around 8–6 Ma i.e. during late Miocene (Fig. 4d). Due to the formation of KT, in the hanging wall, rise in the more topographic front doubled the exhumation rate (~0.52 mma^{-1}) between the KT and the SAT, whereas exhumation rates north of KT (i.e. in the footwall of KT) were slowed down (~0.3 mma^{-1}) between the KT and the NAT (see Table 2).
4. Based on our new ZFT age data and published AFT age data from the Almora klippe, it is clear that tectonics have dominant influence over the post-emplacement exhumation pattern. The abrupt change in FT ages across the MCT (Patel and Carter 2009; Robert et al. 2009; Patel et al. 2011a; Singh et al. 2012) and window zones is described due to duplexing in the footwall of the MCT and reactivation of the MCT in out-of-sequence style during Plio-Quaternary. It is described due to rapid uplift and growth of topography in the MCT hanging wall in HHC zone, and this rapidly exhumed the HHC zone, while the slow uplift of the LHS reflected slow exhumation (Hodges et al. 2004; Wobus et al. 2005; Patel and Carter 2009; Célérier et al. 2009a, b; Patel et al. 2011a, b; Singh et al. 2012). Later on, the reactivation of inner LHD in the inner part of LHS zone and development of MBT imbrication starts the inception of the outer LHD in the outer part of LHS zone during Late Miocene. It causes the young FT ages and rapid exhumation rates in the inner and outer parts of LHS zone (Patel et al. 2015). Based on our results, we suggest that the tectonics have strong control on the uplift and exhumation pattern of the Almora klippe as well as for the LHS zone (Fig. 4e).

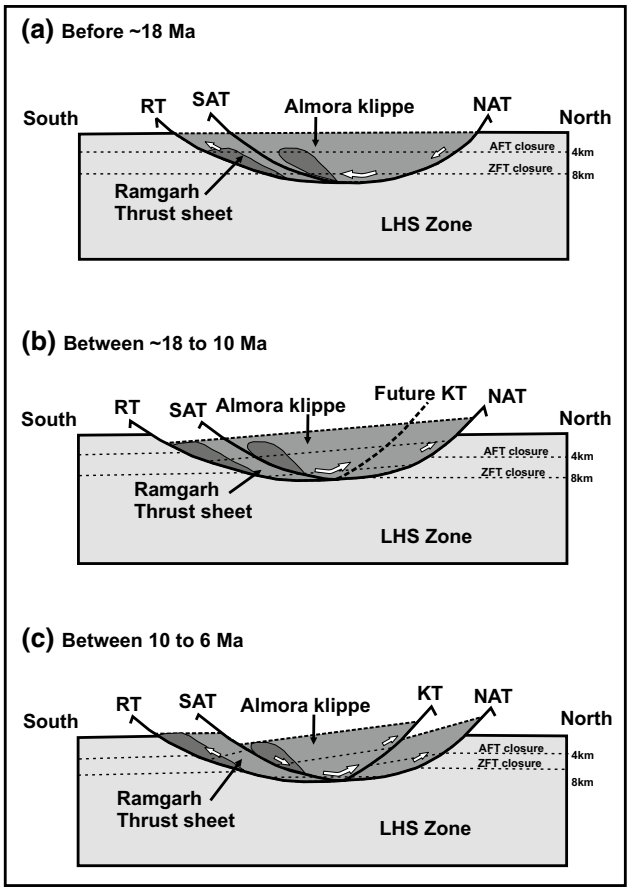

Fig. 5 **a** Schematic diagram showing the post-emplacement structural setting of Almora klippe, **b** reactivation of NAT due to the inception of LHDs, **c** reactivation along the north-dipping Ramgarh Thrust led to uplift of the Ramgarh thrust sheet and synchronous reactivation of the south-dipping KT and NAT in the Almora klippe as back thrusting, and north-dipping SAT as normal faulting (modified after Patel et al. 2015)

Possible kinematics of the Almora–Dadeldhura klippe

Based on the tectonic history and thermochronological data discussed above of the Almora klippe of Kumaun–Garhwal regions of NW Himalaya, we formulate a conceptual model for the post-emplacement kinematics and exhumation history of Almora–Dadeldhura klippe (see Fig. 5). During the Early Miocene or after emplacement of crystalline rocks over the LHS, maximum contraction took place that formed regional synclinal and anticlinal structures. The synclinal part eroded slowly, whereas the anticlinal part quickly (Fig. 5a). Later, it was followed by growth of LHS duplex due to southward propagation of the MHT. The older ZFT ages (~13 Ma) in the hanging wall and close proximity to the NAT illustrated the inception of inner LHD during Middle Miocene and reactivation of the northern Almora–Dadeldhura thrust as a

back thrust (Fig. 5b). Later on the growth of the imbricate structure along with the MBT in outer LHS zone and reactivation of inner LHD initiates the formation of KT as thrust and also reactivate the NAT as back thrust. The young AFT ages (~6 Ma) from the Ramgarh thrust sheet also indicate reactivation of Ramgarh thrust during Late Miocene. Based on our interpretation of FT data, it may be possible that the reactivation the north-dipping RT uplifted the Ramgarh thrust sheet in clockwise direction along a sub-horizontal axis. The space formed by uplift of Ramgarh thrust sheet was compensated by the Almora klippe synchronously by anticlockwise rotation along the same sub-horizontal axis and the south-dipping KT and NAT as back thrust within the Almora klippe during Late Miocene (Fig. 5c).

Conclusions

FT data from the Almora klippe of Kumaun region allow us to constrain the post-emplacement kinematics and exhumation history from Early Miocene to Late Pliocene. The obtained ZFT ages data clearly indicate timing of the development of the LHD in the inner LHS zone and formation of south-dipping KT in the Almora klippe. We conclude that the significant jumps in the AFT ages across the RT, KT and NAT can be linked with the reactivation of these major thrust. Our 1-D thermal modelling exhumation rates also indicate the spatial–temporal variation in exhumation rates of KT-NAT block and SAT-KT block. Our observation shows interaction between spatial and temporal variations in low-temperature thermochronological age data and exhumation rates within the Almora klippen of Kumaun Himalaya, NW India. Our interpretation support the geometry of crustal scale thrust/faults, and their associated kinematics control the topography through uplift and exhumation pathways of rocks. Based on our obtained FT age results and thermal modelling, we conclude that tectonics have strong control over the post-emplacement kinematics and exhumation pattern within the Almora klippen since Middle Miocene.

Acknowledgements PS thanks Prof. A. K. Gupta, Director, Wadia Institute of Himalayan Geology, for his continuous support and encouragement and for providing all requested facilities. Financial support by University Grant Commission research Grant DSKPDF (No. BSR/ES/13-14/0020) was awarded to PS and by Department of Science and Technology, Govt. of India's research Project Nos. SR/S4/ES-341/2008 and IR/S4/ESF-15/2009 was awarded to RCP. SS Bhakuni, WIHG, is acknowledged for fruitful discussion and encouragement. We are grateful to Dr. S. Mukherjee, Associate Editor, for three rounds of detail reviewing and the two anonymous reviewers for critical comments.

References

Antolín B, Godin L, Wemmer K, Nagy C (2013) Kinematics of the Dadeldhura klippe shear zone (W Nepal): implication for the for land evolution of the Himalayan Metamorphic core. Terra Nova 25(4):1–10

Arita K, Shiraishi K, Hayashi D (1984) Geology of the western Nepal and a comparison with Kumaun, India. J Fac Sci Hokkaido Univ IV 21:1–20

Bookhagen B, Burbank DW (2006) Topography, relief, and TRMM-derived rainfall variations along the Himalaya. Geophys Res Lett 33:1–5

Brandon MT, Roden-Tice MK, Garver JI (1998) Late Cenozoic exhumation of the Cascadia accretionary wedge in the Olympic Mountains, northwest Washington State. Geol Soc Am Bull 110:985–1009

Célérier J, Harrison TM, Yin A, Webb AAG (2009a) The Kumaun and Garwhal Lesser Himalaya, India. Part 1: structure and stratigraphy. Geol Soc Am Bull 121:1262–1280

Célérier J, Harrison MT, Beyssac O, Herman F, Dunlap WJ, Webb AAG (2009b) The Kumaun and Garwhal Lesser Himalaya, India: part 2. Thermal and deformation histories. Geol Soc Am Bull 121:1281–1297

Ehlers TA, Chaudhri T, Kumar S, Fuller CW, Willett SD, Ketcham RA, Brandon MT, Belton DX, Kohn BP, Gleadow AJW, Dunai TJ, Fu FQ (2005) Computational tools for low-temperature thermochronometer interpretation. Rev Mineral Geochem 58:589–622

England P, Lefort P, Molnar P, Pecher A (1992) Heat-sources for tertiary metamorphism and anatexis in the Annapurna–Manaslu region central Nepal. J Geophys Res 97:2107–2128

Galbraith RF (1981) On statistical models of fission track count. Math Geol 13:471–488

Godin L, Grujic D, Law RD, Searle MP (2006) Channel flow, extrusion and exhumation in continental collision zones: an introduction. In: Law RD, Searle MP, Godin L (eds) Channel flow, ductile extrusion and exhumation in continental collision zones, vol 268. Geological Society, London, Special Publication, pp 1–23

Heim AA, Gansser A (1939) Central Himalaya: geological observations of the swiss expedition, 1936. Hindu Publications, Delhi, p 26

Herman F, Copeland P, Avouac J-P, Bollinger L, Mahéo G, Le Fort P, Rai S, Foster D, Pêcher A, Stüwe K, Henry P (2010) Exhumation, crustal deformation, and thermal structure of the Nepal Himalaya derived from the inversion of thermochronological and thermobarometric data and modeling of the topography. J Geophys Res 115:B06407

Hodges KV (2000) Tectonics of the Himalaya and southern Tibet from two perspectives. Geol Soc Am Bull 112(3):324–350

Hodges KV, Wobus C, Ruhl K, Schildgen T, Whipple K (2004) Quaternary deformation, river steepening, and heavy precipitation at the front of the Higher Himalayan ranges. Earth Planet Sci Lett 220:379–389

Hurford AJ (1990) Standardization of fission track dating calibration: recommendation by fission track working group of IUGS Subcommission on Geochronology. Chem Geol (Isot Geosci Sec) 80:171–178

Hurford AJ, Green PF (1983) The zeta age calibration of fission-track dating. Chem Geol 41:285–317

Jain AK, Manikvasagam RM (1993) Inverted metamorphism in the intracontinental ductile shear zone during Himalayan collision tectonics. Geology 21:407–410

Johnson MRW, Oliver GJH, Parrish RR, Johnson SP (2001) Synthrusting metamorphism, cooling and erosion of the Himalayan Kathmandu Complex, Nepal. Tectonics 20:394–415

Joshi M (1999) Evolution of the basal shear zone of the Almora klippe, Kumaun Himalaya. In: Jain AK, Manickvasagam RM (eds) Geodynamics of the NW Himalaya, vol 6. Gondwana Research Gp, pp 69–80

Joshi M, Tiwari AN (2008) Structural events and metamorphic consequences in Almora Klippe, during Himalayan Collisional Tectonics. J Asian Earth Sci 34:326–335

Khanal S, Robinson DM, John MJ, Mandal S (2015) Evidence for a far-traveled thrust sheet in the Greater Himalayan thrust system, and an alternative model to building the Himalaya. Tectonics 34:31–52

Long S, McQuarrie N, Tobgay T, Gurjic D (2011) Geometry and crustal shortening of the Himalayan fold-thrust belt, eastern and central Bhutan. Geol Soc Am Bull 123:1427–1447

Mandal S, Robinson DM, Khanal S, Das O (2015) Redefining the tectonostratigraphic and structural architecture of the Almora klippe and Ramgarh Munsiari Thrust in Northwest India. In: Mukherjee S et al. (eds) vol 412. Journal of Geological Society, London, Special Publications, pp 247–269

Molnar P, Tapponier P (1975) Cenozoic tectonics of Asia: effect of continental collision. Science 189:419–425

Mukherjee S (2013a) Channel flow extrusion model to constrain dynamic viscosity and Prandtl number of the Higher Himalaya Shear Zone. Int J Earth Sci 102:1811–1835

Mukherjee S (2013b) Higher Himalaya in the Bhagirathi section (NW Himalaya, India): its structures, backthrusts and extrusion mechanism by both channel flow and critical taper mechanisms. Int J Earth Sci 102:1851–1870

Mukherjee S (2015) A review on out-of-sequence deformation in the Himalaya. In Mukherjee S, Carosi R, van der Beek PA, Mukherjee BK, Robinson DM (eds) Tectonics of the Himalaya, vol 412. Geological Society, London, Special Publication, pp 67–109

Mukherjee S, Koyi HA (2010a) Higher Himalayan Shear Zone, Sutlej section—structural geology and extrusion mechanism by various combinations of simple shear, pure shear and channel flow in shifting modes. Int J Earth Sci 99:1267–1303

Mukherjee S, Koyi HA (2010b) Higher Himalayan Shear Zone, Zanskar section—microstructural studies and extrusion mechanism by a combination of simple shear and channel flow. Int J Earth Sci 99:1083–1110

Mukherjee S, Koyi HA, Talbot CJ (2012) Implications of channel flow analogue models for extrusion of the Higher Himalayan Shear Zone with special reference to the out-of sequence thrusting. Int J Earth Sci 101:253–272

Naeser CW (1979) Fission-track dating and geological annealing of fission tracks. In: Jager E, Hunziker JC (eds) Lecture in isotope geology. Springer, Heidelberg, New York, p 154

Patel RC, Carter A (2009) Exhumation history of the Higher Himalayan Crystalline along Dhauliganga–Goriganga River valleys, NW India: new constraints from fission-track analysis. Tectonics. doi:10.1029/2008TC002373

Patel RC, Kumar Y, Lal N, Kumar A (2007) Thermotectonic history of the Chiplakot Crystalline Belt in the Lesser Himalaya, Kumaun, India: constraints from apatite fission-track thermochronology. J Asian Earth Sci 29:430–439

Patel RC, Adlakha V, Lal N, Singh P, Kumar Y (2011a) Spatiotemporal variation in exhumation of the Crystallines in the NW-Himalaya, India: constraints from fission track dating analysis. Tectonophysics 504(1–4):1–13

Patel RC, Adlakha V, Singh P, Kumar Y, Lal N (2011b) Geology, structural and exhumation history of the Higher Himalayan Crystallines in Kumaun Himalaya, India. J Geol Soc India 77(1):47–72

Patel RC, Singh P, Lal N (2015) Thrusting and back-thrusting as post-emplacement kinematics of the Almora klippe: insights from low-temperature thermochronology. Tectonophysics 653:41–51

Rao DR, Sharma R, Patel RC, Bhakuni SS (2014) Metamorphism and P–T estimates of the Higher Himalayan Crystallines (HHC) of Kaliganga Valley, NE Kumaun Himalaya, India. Himal Geol 35(2):171–181

Ray L, Bhattacharya A, Roy S (2007) Thermal conductivity of Higher Himalayan Crystallines from Garhwal Himalaya, India. Tectonophysics 434(1–4):71–79

Reiners PW, Brandon MT (2006) Using thermochronology to understand orogenic erosion. Ann Rev Earth Planet Sci 34:419–466

Reiners PW, Spell TL, Nicolescu S, Zanetti KA (2004) (U–Th)/He thermochronometry: He diffusion and comparison with $^{40}Ar/^{39}Ar$ dating. Geochim Cosmochim Acta 68:1857–1887

Reiners PW, Ehlers TA, Zeitler PK (2005) Past, Present and Future of thermochronology. In Reiners PW, Ehlers TA (Eds) Low-temperature thermochronology: techniques, interpretations, and applications, vol 58. Reviews in Mineralogy Geochemistry, pp 1–18

Robert X, van der Beek P, Braun J, Perry C, Dubille M, Mugnier J-L (2009) Assessing Quaternary reactivation of the Main Central thrust zone (central Nepal Himalaya): new thermochronologic data and numerical modeling. Geology 37:731–734

Robert X, van der Beek P, Braun J, Perry C, Mugnier J-L (2011) Control of detachment geometry on lateral variations in exhumation rates in the Himalaya: insights from low-temperature thermochronology and numerical modelling. J Geophy Res 116:B05202

Robinson DM, McQuarrie N (2012) Pulsed deformation and variable slip rates within the central Himalayan thrust belt. Lithosphere 4(5):449–464

Robinson DM, Pearson ON (2006) Exhumation of Greater Himalayan rock along the Main Central Thrust in Nepal: implications for channel flow. In: Law RD, Searle MP, Godin L (Eds.) Channel flow, ductile extrusion and exhumation in continental collision zones, vol 268. Geological Society, London, Special Publication, pp 255–267

Robinson DM, Pearson OP (2013) Was Himalayan normal faulting triggers by initiation of the Ramgarh–Munsiari Thrust? Int J Earth Sci 102(7):1773–1790

Robinson DM, Decelles PG, Garzione CN, Pearson ON, Harrison TM, Catlos EJ (2003) Kinematic model for the Main Central thrust in Nepal. Geology 31(4):359–362

Robinson DM, DeCelles PG, Copeland P (2006) Tectonics evolution of the Himalayan Thrust belt in western Nepal: implication for channel flow models. Geol Soc Am Bull 118:865–885

Roy S, Rao RUM (2000) Heat flow in the Indian shield. J Geophys Res 105(B11):25587–25604

Rupke J (1974) Stratigraphic and structural evolution of the Kumaun Lesser Himalaya, Himachal Pradesh, India. In: Flugel E (ed) Fossil algae. Springer, Berlin, pp 86–100

Sakai H, Iwano H, Danhara T, Hirata T, Takigami T (2013) Emplacement of hot Lesser Himalayan nappes from 15 to 10 Ma in the Jumla–Surkhet region, western Nepal, and their thermal imprint on the underlying Early Miocene fluvial Dumri Formation. Island Arc 22:361–381

Searle MP, Windley BF, Coward MP, Cooper DJW, Rex AJ, Rex D, Tingdong L, Xudhang X, Jan MQ, Thakur CC, Kamar S (1987) The closing of Tethys and the tectonics of the Himalaya. Geol Soc Am Bull 98:678–701

Singh P, Patel RC, Lal N (2012) Plio-Plistocene in-sequence thrust propagation along the Main Central Thrust zone (Kumaun–Garhwal Himalaya, India): new thermochronological data. Tectonophysics 574–575:193–203

Spencer CJ, Harris RA, Dorais MJ (2012) Depositional provenance of the Himalayan metamorphic core of Garhwal region, India: constrained by U–Pb and Hf isotopes in zircons. Gondwana Res 22(1):26–35

Srivastava P, Mitra G (1994) Thrust geometries and deep structure of the outer and lesser Himalaya, Kumaun and Garhwal (India): implications for evolution of the Himalayan fold-and-thrust belt. Tectonics 13:89–109

Srivastava P, Mitra G (1996) Deformation mechanisms and textures in mylonites along the North Almora thrust (Kumaun Himalayas, India): evidence for heterogeneous deformation and conductive cooling during thrusting. J Struct Geol 18:27–39

Thiede RC, Ehlers TA, Bookhagen B, Strecker MR (2009) Erosional variability along the NW Himalaya. J Geophys Res 114:F01015

Upreti BN, LeFort P (1999) Lesser Himalayan crystalline nappes of Nepal: problems of their origin. Geol Soc Lond Spec Publ 328:225–238

Valdiya KS (1962) An outline of the structure and stratigraphy of the southern part of the Pithoragarh District UP. J Geol Soc India 3:27–48

Valdiya KS (1980a) Geology of the Kumaun Lesser Himalaya. Wadia Institute of Himalayan Geology, Dehradun, p 291

Valdiya KS (1980b) The two intracrustal boundary thrusts of the Himalaya. Tectonophysics 66:323–348

Valdiya KS (1986) Neotectonic activities in the Himalayan belt. In: Proceedings of international symposium neotectonics in South Asia, Dehradun, Survey of India, pp 241–267

Valdiya KS (2001) Reactivation of terrane-defining boundary thrusts in central sector of the Himalaya: implications. Curr Sci 81(11):1418–1430

Valdiya KS, Kotlia BS (2001) Fluvial geomorphic evidence for later Quaternary reactivation of a synclinally folded klippe in Kumaun Lesser Himalaya. J Geol Soc India 58:303–317

Valdiya KS, Kotlia BS, Pant PD, Shah M, Mungali N, Tewari S, Shah N, Upreti M (1996) Quaternary palaeolakes in Kumaun Lesser Himalaya: finds of neotectonic and palaeoclimatic significance. Curr Sci 70(2):157–160

van der Beek P, Litty C, Baudin M, Mercier J, Robert X, Hardwick E (2016) Contrasting tectonically driven exhumation and incision patterns, western versus central Nepal Himalaya. Geology 44(4):327–330

Webb AAG (2013) Preliminary balanced palinspastic reconstruction of Cenozoic deformation across the Himachal Himalaya (northwestern India). Geosphere 9(3):572–587

Webb AAG, Yin A, Harrison TM, Célérier J, Burgess WP (2007) The leading edge of the Greater Himalayan Crystalline complex revealed in the NW Indian Himalaya: implications for the evolution of the Himalayan orogeny. Geology 35(10):955–958

Webb AAG, Yin A, Harrison TM, Célérier J, Gehrels GE, Manning CE, Grove M (2011) Cenozoic tectonic history of the Himachal Himalaya (northwestern India) and its constraints on the formation mechanism of the Himalayan orogen. Geosphere 7:1013–1061

Whipp DM Jr, Ehlers TA, Blythe AE, Huntington KW, Hodges KV, Burbank DW (2007) Plio-Quaternary exhumation history of the central Nepalese Himalaya: 2 thermokinematic and thermochronometer age prediction model. Tectonics 26:TC3003

Wobus C, Heimsath A, Whipple K, Hodges K (2005) Active out-of-sequence thrust faulting in the central Nepalese Himalaya. Nature 434:1008–1011